Rapid SiO_2 Atomic Layer Deposition Using Tris(*tert*-pentoxy)silanol

B. B. Burton,[†] M. P. Boleslawski,[‡] A. T. Desombre,[‡] and S. M. George*[,†,§]

Department of Chemistry and Biochemistry and Department of Chemical and Biological Engineering, University of Colorado, Boulder, Colorado 80309, and SAFC Hitech, Sheboygan Falls, Wisconsin 53085

Received June 26, 2008. Revised Manuscript Received September 6, 2008

Rapid SiO_2 atomic layer deposition (ALD) can deposit very thick and conformal SiO_2 films by silanol exposure to surfaces covered with Al catalysts. In this study, we have explored the growth of rapid SiO_2 ALD films using liquid tris(*tert*-pentoxy)silanol (TPS). The SiO_2 film thicknesses were determined using quartz crystal microbalance and X-ray reflectivity measurements. The SiO_2 film thicknesses deposited during one silanol exposure were dependent on the substrate temperature, silanol pressure, and silanol exposure time. The dependence of the SiO_2 growth on these parameters helped to establish the mechanism of rapid SiO_2 ALD. For TPS exposures of 1 s, the SiO_2 ALD growth rate was larger at lower temperatures and higher TPS pressures. SiO_2 ALD thicknesses of 125−140 Å were observed at the highest TPS pressures of ∼1 Torr at lower temperatures of 150 and 175 °C. Rapid SiO_2 ALD is believed to result from the growth of siloxane polymer chains at the Al-catalytic sites and the cross-linking of these polymer chains to form a dense SiO_2 film. The results indicated that higher TPS fluxes increase the siloxane polymerization rates. Likewise, the lower temperatures reduce the cross-linking rates between the siloxane polymers that self-limit the SiO_2 deposition. To explore the rate of cross-linking between the siloxane polymers, experiments were conducted where small TPS micropulses were employed with different delay times between the micropulses. The SiO_2 ALD thicknesses decreased with increasing delay times. This behavior suggested that the longer delay times produced more cross-linking that self-limits the SiO_2 deposition. Other experiments showed that higher temperatures produced faster nucleation of the rapid SiO_2 ALD. The nucleation was nearly immediate at the higher temperatures and could be as long as 10 s at the lower temperatures. The growth kinetics of rapid SiO_2 ALD can be understood in terms of the temperature dependence of nucleation and cross-linking and the pressure dependence of the siloxane polymerization rate. Rapid SiO_2 ALD was also dependent on the presence of pyridine derivatives in the TPS. These Lewis base impurities catalyze both the initial nucleation and the cross-linking reaction during rapid SiO_2 ALD.

I. Introduction

Atomic layer deposition (ALD) is a thin-film growth method based on sequential, self-limiting surface reactions.[1] ALD can be used to grow ultrathin and conformal films of a wide variety of materials including oxides, nitrides, and metals.[1,2] Silicon dioxide (SiO_2) is the most common dielectric material in silicon microelectronic devices.[3] Despite its importance, SiO_2 ALD has been difficult. SiO_2 ALD using $SiCl_4$ and H_2O requires high temperatures of >325 °C and large reactant exposure of $>10^9$ L (1 L = 10^{-6} Torr s).[4−7] However, catalyzed SiO_2 ALD can be accomplished using Lewis bases at temperatures close to room temperature and much smaller exposures.[8−12]

Silicon precursors besides $SiCl_4$ have been utilized for SiO_2 ALD. These other thermal chemistry approaches have required long reactant exposure times and include $Si(NCO)_4$ and H_2O,[13] $(H_3CO)Si(NCO)_3$ and H_2O_2,[14] and $Si(NCO)_4$ and $N(C_2H_5)_3$.[15] Ozone has also been employed for SiO_2 ALD with SiH_2Cl_2 at 300 °C and required reactant exposures $>10^9$ L.[16] In addition, the use of O_2/N_2 plasma with $ClSi(N(CH_3)_2)_3$ and $Si(N(CH_3)_2)_4$ yielded SiO_2 ALD films at 100−250 °C.[17] Another approach for controlled SiO_2 growth was based on the self-limiting adsorption of tris(*tert*-butoxy)silanol (TBS) at 25 °C and resulted in ∼10 Å thick SiO_2 films on Si(100).[18]

[†] Department of Chemistry and Biochemistry, University of Colorado.
[‡] SAFC Hitech.
[§] Department of Chemical and Biological Engineering, University of Colorado.

(1) George, S. M.; Ott, A. W.; Klaus, J. W. *J. Phys. Chem.* **1996**, *100*, 13121.
(2) Ritala, M.; Leskela, M. *Handbook of Thin Film Materials*; Academic Press: San Diego, CA,2001.
(3) Wolf, S.; Tauber, R. N. *Silicon Processing for the VLSI Era, Process Technology*; Lattice Press: Sunset Beach, CA, 1986.
(4) Ferguson, J. D.; Weimer, A. W.; George, S. M. *Chem. Mater.* **2000**, *12*, 3472.
(5) Ferguson, J. D.; Weimer, A. W.; George, S. M. *Appl. Surf. Sci.* **2000**, *162*, 280.
(6) Klaus, J. W.; Ott, A. W.; Johnson, J. M.; George, S. M. *Appl. Phys. Lett.* **1997**, *70*, 1092.
(7) Sneh, O.; Wise, M. L.; Ott, A. W.; Okada, L. A.; George, S. M. *Surf. Sci.* **1995**, *334*, 135.
(8) Du, Y.; Du, X.; George, S. M. *Thin Solid Films* **2005**, *491*, 43.
(9) Du, Y.; Du, X.; George, S. M. *J. Phys. Chem. C* **2007**, *111*, 219.
(10) Klaus, J. W.; George, S. M. *Surf. Sci.* **2000**, *447*, 81.
(11) Klaus, J. W.; Sneh, O.; George, S. M. *Science* **1997**, *278*, 1934.
(12) Klaus, J. W.; Sneh, O.; Ott, A. W.; George, S. M. *Surf. Rev. Lett.* **1999**, *6*, 435.
(13) Gasser, W.; Uchida, Y.; Matsumura, M. *Thin Solid Films* **1994**, *250*, 213.
(14) Morishita, S.; Uchida, Y.; Matsumura, M. *Jpn. J. Appl. Phys., Part 1* **1995**, *34*, 5738.
(15) Yamaguchi, K.; Imai, S.; Ishitobi, N.; Takemoto, M.; Miki, H.; Matsumura, M. *Appl. Surf. Sci.* **1998**, *132*, 202.
(16) Lee, J. H.; Kim, U. J.; Han, C. H.; Rha, S. K.; Lee, W. J.; Park, C. O. *Jpn. J. Appl. Phys., Part 2* **2004**, *43*, L328.
(17) Lim, J. W.; Yun, S. J.; Lee, J. H. *ETRI J.* **2005**, *27*, 118.

10.1021/cm801738z CCC: $40.75
Published on Web 10/30/2008

Recently, a new SiO_2 deposition method using silanols with Al catalysts has been developed that is known as rapid SiO_2 ALD.[19,20] Rapid SiO_2 ALD produces deposition rates >100 times larger than conventional SiO_2 ALD while still maintaining the self-limiting behavior characteristic of ALD.[19] Silanols used for rapid SiO_2 ALD include TBS and tris(*tert*-pentoxy)silanol (TPS). Rapid SiO_2 ALD using TBS deposited SiO_2 layers with thicknesses up to ~120 Å in one silanol exposure.[19] The maximum growth rate of 120 Å was obtained at 225−250 °C, and the growth rate decreased at both higher and lower deposition temperatures.[19] Rapid SiO_2 ALD required a catalyst on the surface in the form of aluminum from trimethyl aluminum (TMA).[19] However, other metals such as hafnium and zirconium have also been used as the catalyst for rapid SiO_2.[21−23]

In this study, rapid SiO_2 ALD was performed using TPS with TMA providing the Al catalyst. TPS is a volatile liquid that yields some delivery advantages compared with the solid TBS. The investigations explored the growth kinetics and mechanism for rapid SiO_2 ALD. In situ quartz crystal microbalance (QCM) investigations determined the dependence of deposition temperature and TPS exposure pressure on rapid SiO_2 ALD growth. Ex situ X-ray reflectometry (XRR) analysis confirmed the growth rates and also determined the density and relative roughness of the rapid SiO_2 ALD films. Exposure experiments were conducted where small TPS micropulses were employed with different delay times between the micropulses. These investigations helped reveal the self-limiting mechanism for rapid SiO_2 ALD. The impurity tris(*tert*-pentoxy)silylpyridine was also observed to have a catalytic effect on rapid SiO_2 ALD.

II. Experimental Section

Rapid SiO_2 ALD was performed from 125−300 °C in a viscous-flow ALD reactor[24] using TPS and TMA. A top view of the viscous flow reactor equipped with the QCM sensor is shown schematically in Figure 1. Nitrogen was used as a carrier gas on the H_2O and TMA lines. The total N_2 flow rate was 150 sccm, and this flow rate produced a pressure of 0.5 Torr in the reactor. The reactants were TMA (Strem, 98%), H_2O (Fischer Scientific, Optima purity), and TPS (SAFC Hitech, 99.99%). Other potential precursors investigated for rapid SiO_2 included TBS (SAFC Hitech, 99.999%) and tris(isopropoxy)silanol (TIS) (SAFC Hitech, 99.999%).

The TPS was held in a stainless steel bubbler and maintained between 75−150 °C to obtain a range of vapor pressures. The TMA was contained in a gas cylinder and was maintained at room temperature. The H_2O was held in a glass coldfinger and also maintained at room temperature. All chemicals were used as received. Various batches of TPS were also investigated with known concentrations of tris(*tert*-pentoxy)silylpyridine obtained from two different synthetic routes. The first route could produce tris(*tert*-pentoxy)silylpyridine concentrations of 310 ppm, 78 ppm, and ~0 ppm. Unless otherwise noted, the TPS batch with ~0 ppm was used for all experimental investigations. Another synthetic route that prevents the formation of tris(*tert*-pentoxy)silylpyridine yielded TPS with 0 ppm of tris(*tert*-pentoxy)silylpyridine. These reactants were all obtained from SAFC Hitech.

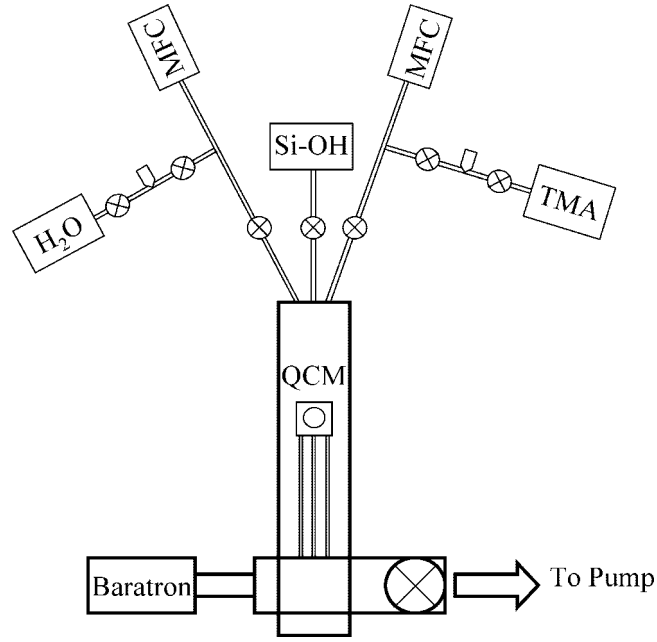

Figure 1. Schematic of viscous flow ALD reactor equipped with QCM sensor.

The reactor was equipped with computer-controlled pneumatic dose valves for controlled precursor deposition and a Baratron capacitance manometer for pressure measurements. Alternating exposures of TMA and TPS were used for rapid SiO_2 ALD. Hereafter, the ALD reactant pulse timing sequence is given by $t_1-t_2-t_3-t_4$ where t_1 is the exposure time for TMA, t_2 is the purge following the TMA exposure, t_3 is the TPS exposure, and t_4 is the purge following the TPS exposure. All exposure times are given in seconds. Three different TPS dosing schemes were investigated: single exposure; multiple exposures; and continuous exposure. These schemes will be discussed in more detail later.

QCM measurements were used for in situ analysis of rapid SiO_2 ALD. The QCM setup has been described previously.[24,25] Briefly, a Maxtek TM 400 thin-film deposition monitor measured the QCM oscillation frequency. Polished QCM sensors with a resonant frequency of ~6 MHz were obtained from Colorado Crystal Corporation (Longmont, CO). The QCM sensors were mounted in a Maxtek BSH-150 bakeable sensor head positioned in the center of the reactor and attached to a 2.75 in. Conflat flange. The QCM was equipped with a backside purge to prevent deposition on the back side of the QCM crystal.[24] The QCM apparatus has a mass resolution of 0.3 ng/cm^2 when the temperature is stable to within ±0.1 °C. The temperature was controlled with a Eurotherm temperature controller model 2604.

Rapid SiO_2 ALD was also performed on Si(100) wafers. The Si(100) wafers were used for X-ray reflectivity (XRR), Rutherford backscattering (RBS), and secondary ion mass spectrometry (SIMS) analysis. The Si(100) wafers were dipped in 1% HF for 60 s

(18) Miller, K. A.; John, C.; Zhang, K. Z.; Nicholson, K. T.; McFeely, F. R.; Holl, M. M. B. *Thin Solid Films* **2001**, *397*, 78.
(19) Hausmann, D.; Becker, J.; Wang, S. L.; Gordon, R. G. *Science* **2002**, *298*, 402.
(20) de Rouffignac, P.; Li, Z. W.; Gordon, R. G. *Electrochem. Solid-State Lett.* **2004**, *7*, G306.
(21) Zhong, L. J.; Daniel, W. L.; Zhang, Z. H.; Campbell, S. A.; Gladfelter, W. L. *Chem. Vap. Deposition* **2006**, *12*, 143.
(22) Zhong, L. J.; Zhang, Z. H.; Campbell, S. A.; Gladfelter, W. L. *J. Mater. Chem.* **2004**, *14*, 3203.
(23) He, W.; Solanki, R.; Conley, J. F.; Ono, Y. *J. Appl. Phys.* **2003**, *94*, 3657.
(24) Elam, J. W.; Groner, M. D.; George, S. M. *Rev. Sci. Instrum.* **2002**, *73*, 2981.
(25) Fabreguette, F. H.; Sechrist, Z. A.; Elam, J. W.; George, S. M. *Thin Solid Films* **2005**, *488*, 103.

followed by a standard RCA-1 ($NH_4OH:H_2O_2:H_2O = 1:1:5$) clean and rinse. The Si(100) wafers were covered with a chemical oxide of ~30 Å. Samples were held for at least 30 min in the viscous flow reactor prior to rapid SiO_2 ALD.

The XRR scans were performed at the University of Colorado using a Bede D1 high resolution X-ray diffractometer from Bede Scientific Inc. This X-ray diffractometer was equipped with a Cu X-ray tube working at $\lambda = 1.54$ Å. The filament current was 40 mA, and the voltage was 40 kV. Raw data were fit using REFS fitting software from Bede Scientific Inc. The XRR fits revealed the film thicknesses, film densities, and surface roughness.

The FTIR studies were conducted in another vacuum reactor that has been utilized in previous experiments.[26] The FTIR investigations were conducted in the upper chamber of the reactor. The upper chamber was equipped with computer-controlled pneumatic dose valves and a Baratron capacitance manometer for pressure measurement. The upper chamber was also pumped with a two-stage rotary pump. The mechanical pump maintained a pressure of 0.5 Torr with a continuous Nitrogen flow of 100 sccm into the upper chamber. The lower chamber of the reactor was maintained at a pressure of 2×10^{-9} Torr using a turbomolecular pump with a pumping speed of 56 L/s.

High surface area particles were required for transmission FTIR spectroscopy studies.[26] The ZrO_2 particles used in this experiment were spherical with an average diameter of 50 nm and a surface area of ~20.2 m^2/g. These ZrO_2 particles were obtained from Nanomaterials Research Corporation (Longmont, CO). The particles were supported on a photoetched tungsten grid as described in previous investigations.[26−28] The FTIR studies were performed with a Nicolet Magna 560 FTIR spectrometer equipped with a nitrogen-cooled MCT-B infrared detector.[26] The spectrometer setup was purged with dry, CO_2-free air, delivered from a purge gas generator. Spectra were collected with a mirror speed of 3.6 $cm \cdot s^{-1}$ and averaged over 200 scans using 4 cm^{-1} resolution. All spectra were normalized using the background of the reactor prior to the insertion of the tungsten grid.

During FTIR experiments, sequential exposures of TMA and H_2O were used first to deposit a 1 nm seed layer of Al_2O_3 on the ZrO_2 particles at 150 °C. This Al_2O_3 ALD layer ensures the reproducibility of the initial surface. Subsequently, exposures of TMA and TPS were used to deposit 1 cycle of rapid SiO_2 ALD. The TPS was held in a stainless steel bubbler at 82 °C. The TPS partial pressure was 25 mTorr. The precursor forelines were heated to 100 °C to prevent TPS condensation.

The RBS and elastic recoil detection (ERD) analysis were performed at the facility for Ion Beam Analysis of Materials (IBeAM) in the LeRoy Eyring Center for Solid State Science at Arizona State University. The RBS and ERD scans were obtained using a General Ionex Tandetron ion accelerator. A He^{2+} source ion energy of 2 MeV was used for RBS. ERD is more sensitive to lighter elements and was used for the detection of hydrogen. For ERD analysis, the detector is placed in a forward scattering position, and the He^{2+} source ion energy was 1.8 MeV.

Secondary ion mass spectrometry (SIMS) was conducted by the Evans Analytical Group. For aluminum investigations, SIMS analysis was performed on an Atomika 4500 quadrupole tool with a 1 keV O_2 primary beam while detecting positive secondary ions. For nitrogen investigations, SIMS analysis was performed on an Atomika 4100 quadrupole tool with a 3 keV Cs primary beam while detecting negative secondary ions. Considering the mass interference of $^{28}Si^{14}N$ and $^{30}Si^{12}C$ at mass 42, the intensity of $^{28}Si^{12}C$ was measured, and the corresponding intensity of $^{30}Si^{12}C$ was determined based on the isotopic abundances of ^{28}Si (92.2%) and ^{30}Si (3.1%). The contribution from $^{30}Si^{12}C$ was then subtracted from the total intensity at mass 42 to obtain the intensity of $^{28}Si^{14}N$.

III. Results and Discussion

A. Initial Studies with Different Silanol Precursors. The previous study measured a growth per cycle of 120 Å using TBS at 225−250 °C.[19] Initial experiments attempted to reproduce these results. However, a large dependence on the exposure pressure was observed during these experiments. Precursor condensation was also observed in the lines and valves because TBS is a solid. Both TIS and TPS were also investigated to alleviate some of the problems of working with a solid precursor. TIS is a liquid and has the highest vapor pressure of the silanol compounds commercially available. However, TIS did not illustrate rapid SiO_2 ALD behavior between 125 and 250 °C. TPS is also a liquid precursor. Initial investigations of TPS observed rapid SiO_2 ALD at much lower deposition temperatures and higher deposition rates than previously observed using TBS. TPS was determined to be the most suitable precursor for further investigations of rapid SiO_2 ALD.

B. Single Exposure Experiments. The timing sequence during TPS experiments with single 1 s exposures was 2−30−1−120. The same conditions were used for both QCM and XRR investigations. A 2 s TMA exposure initiated the timing sequence. After a 30 s purge, the substrates were exposed to a TPS exposure for 1 s. The partial pressure of the TPS was controlled by elevating the bubbler temperature from 75−150 °C. This temperature range led to partial pressures of TPS from 10 mTorr to 2.5 Torr. The TPS was attached directly on the reactor to avoid dilution of the precursor. However, the N_2 carrier gas was flowing through the H_2O and TMA lines during the TPS exposures.

The QCM monitored the mass gain per cycle versus TPS pressure and substrate temperature from 150−250 °C using single TPS exposures of 1 s. A summary of these results is shown in Figure 2. The density of ~2.0 g/cm^3 obtained from ex situ XRR analysis of the rapid SiO_2 ALD films was used to determine the corresponding film thickness from the QCM mass gains. These film thicknesses are displayed on the right axis of Figure 2. The highest growth rate of ~140 Å/cycle was observed at 150 °C with ~1 Torr reactant exposures. The maximum mass gain for TPS dropped progressively at higher substrate temperatures. These results are different than the results obtained using TBS that had a maximum growth per cycle of 120 Å that was peaked at 225−250 °C.[19]

The mass gains shown in Figure 2 were very dependent on the TPS pressure at each substrate temperature. The mass gains were nearly linear with TPS pressure. However, this trend appeared to self-limit at the lower temperatures with ~1 Torr exposures. The mass gains observed at lower TPS pressures at 150−175 °C also illustrated nonlinearity close to the origin that is partially obscured in Figure 2. The smaller deposition rates at the lowest TPS pressures are attributed

(26) Ferguson, J. D.; Weimer, A. W.; George, S. M. *Thin Solid Films* **2000**, *371*, 95.
(27) Ferguson, J. D.; Weimer, A. W.; George, S. M. *Thin Solid Films* **2002**, *413*, 16.
(28) Ferguson, J. D.; Weimer, A. W.; George, S. M. *Chem. Mater.* **2004**, *16*, 5602.

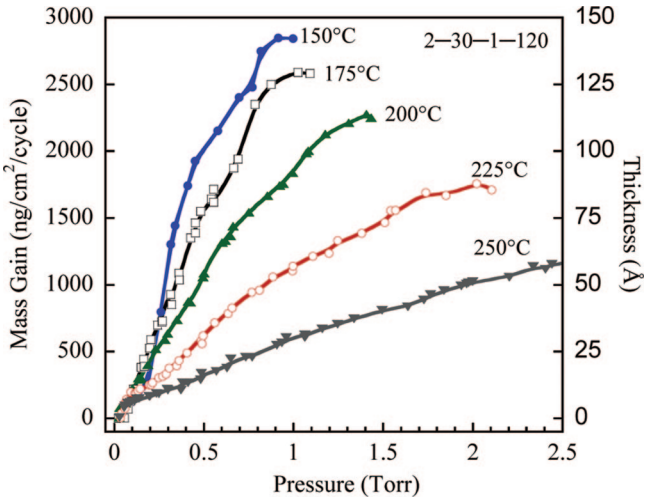

Figure 2. Summary of mass gains for various substrate temperatures for single TPS exposures of 1 s at various TPS pressures.

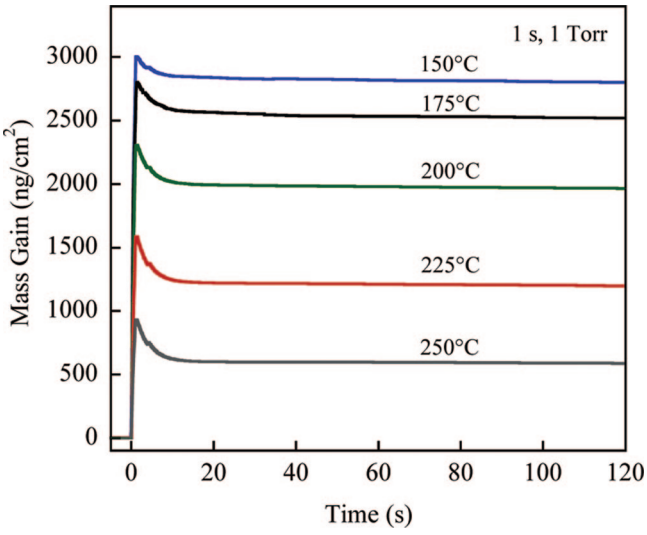

Figure 3. Mass gain versus time for various substrate temperatures for single TPS exposures of 1 s at a TPS pressure of 1 Torr.

to the delayed nucleation of rapid SiO_2 ALD at lower temperatures and will be discussed later.

Figure 3 displays the QCM signals versus time for different substrate temperatures for the TPS exposures of 1 s at the same pressure of ~1 Torr. As expected from Figure 2, the largest mass gains were observed for the lowest temperatures. In addition, the largest subsequent mass losses after the reactant absorption were observed at the highest temperatures. For example, at 150 °C the mass gain was 3010 ng/cm^2 and the subsequent mass loss was 200 ng/cm^2. This mass gain and loss led to an overall mass deposition of 2810 ng/cm^2. Conversely, at 250 °C the mass gain was 928 ng/cm^2 and the subsequent mass loss was 387 ng/cm^2, yielding an overall mass deposition of 541 ng/cm^2.

These QCM results yield some insight into the growth mechanism during rapid SiO_2 ALD using TPS. The main steps in the growth mechanism are shown in Figure 4. The rapid SiO_2 ALD is believed to occur via siloxane polymerization.[19,29] First, TMA reacts with available hydroxylated sites as given by the reaction in eq 1. Subsequently, the silanols react at the Al center to release CH_4 as expressed by the reaction in eq 2.

$$SiOH^* + Al(CH_3)_3 \rightarrow SiOAl(CH_3)_2^* + CH_4 \quad (1)$$

$$SiOAlCH_3^* + (CH_3CH_2(CH_3)_2CO)_3SiOH \rightarrow SiOAlOSi(OC(CH_3)_2CH_2CH_3)_3^* + CH_4 \quad (2)$$

Additional silanol precursors then can insert at the Al catalytic center and release *tert*-pentanol as given by the reaction eq 3.

$$SiOAlOSi(OC(CH_3)_2CH_2CH_3)_3^* + (CH_3CH_2(CH_3)_2CO)_3SiOH \rightarrow SiOAlOSi(OC(CH_3)_2CH_2CH_3)_2—O—Si(OC(CH_3)_2CH_2CH_3)_3^* + (CH_3)_3CCH_2OH \quad (3)$$

The polymerization reaction is believed to occur as long as the silanol precursors can diffuse to the Al catalyst.[19] Cross-linking reactions between the siloxane chains are in competition with the silanol diffusion. First, the *tert*-pentoxy ligands eliminate isopentylene and leave behind hydroxyl groups as expressed by the reaction eq 4.

$$—OSi(OC(CH_3)_2CH_2CH_3)_3^* \rightarrow —OSiOH^* + H_2C{=}CCH_3CH_2CH_3 \quad (4)$$

The hydroxyl groups can subsequently react with other hydroxyl groups to yield H_2O and cross-linking siloxane bonds that terminate the SiO_2 growth as given by the reaction eq 5.

$$2SiOH^* \rightarrow Si—O—Si + H_2O \quad (5)$$

After the polymerization reaction stops, TMA is redeposited on the SiO_2 surface to repeat the rapid SiO_2 ALD reaction sequence.

Figure 3 illustrates that the mass gains were much larger at lower temperatures. This behavior indicates the propagation of the siloxane chains by the reaction in eq 3 was faster relative to the cross-linking of the siloxane chains by the reaction in eq 5 at lower temperatures. The larger relative rates of propagation may result from the activation barriers for diffusion of the incoming TPS precursors and the cross-linking reaction. A larger activation barrier for the cross-linking reaction would lead to larger relative propagation rates of the siloxane chains at lower temperatures. In addition, Figure 3 shows that the subsequent mass loss after the peak mass gain was also lowest at the lower temperatures. These lower mass losses are attributed to the slower desorption of both reaction products and unreacted TPS that was unable to reach the Al catalytic centers.

The XRR results confirmed the growth rates observed by QCM from 150−250 °C. An initial nucleation period of ~2−3 cycles was observed when using single exposures on a starting Al_2O_3 ALD surface. Typically, the first rapid SiO_2 ALD cycle would only deposit 50% of the growth per cycle obtained in steady state after four to five cycles. The second and third cycles of rapid SiO_2 ALD would deposit between 75−90% of the growth per cycle obtained in steady state. Thereafter, each cycle would deposit the SiO_2 ALD growth

(29) Gaul, J. H.; Carr, T. M. *Spectrosc. Lett.* **1983**, *16*, 651.

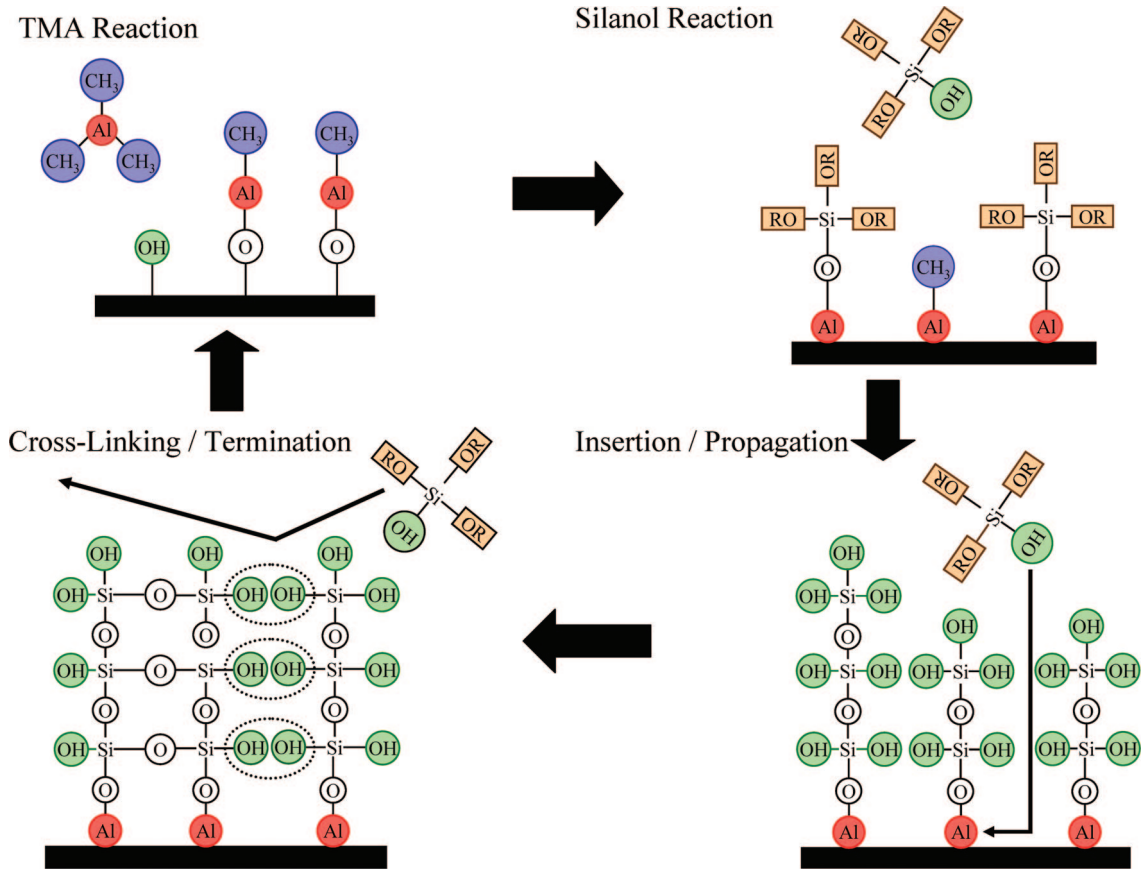

Figure 4. Main steps in the growth mechanism of rapid SiO_2 ALD.

per cycle predicted by the QCM results shown in Figure 2. The SiO_2 ALD films were fairly rough using the single exposure conditions. The SiO_2 ALD film roughness scaled approximately with the square root of the film thickness as expected for a random deposition process.[30] Consequently, the XRR studies had difficulty obtaining accurate thickness measurements for SiO_2 ALD films with thicknesses > 1200 Å.

C. Multiple Exposure Experiments with Variable Delay Times. To further understand the mechanism of rapid SiO_2 ALD, additional experiments were conducted that utilized multiple TPS micropulses. These micropulses were defined by TPS exposures that were significantly less than the exposures required for the reactions to reach completion. In addition, a variable delay time was defined between the micropulses. These experiments were performed for both an $AlCH_3$* methyl-terminated surface and an AlOH* hydroxyl-terminated surface.

The timing sequence on the AlOH* surface was 2−30−2−30−(15(1, d)), where d is the delay time that was 30, 45, and 90 s. To explain further, a 2 s TMA exposure was followed by a 30 s purge. Next, a 2 s H_2O exposure was followed by a 30 s purge. Lastly, there were fifteen 1 s micropulses of TPS that were separated by a delay time of either $d = 30$ s, 45 s, or 90 s. The H_2O exposure was left out for the $AlCH_3$* surface, and the timing sequence was 2−30−(15 (1, d)). For all of these experiments, the partial pressure of TPS was 300 mTorr. These experiments were all conducted at 175 °C.

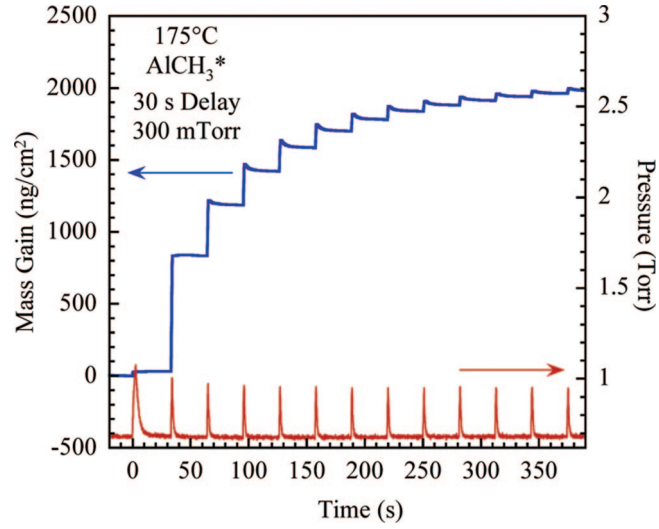

Figure 5. Mass gain versus time for a multiple series of undersaturating TPS micropulses on an $AlCH_3$* surface at 175 °C with a 30 s delay between the TPS micropulses. The pressure during each TPS micropulse is 300 mTorr.

Figure 5 shows the mass gain versus time for a multiple series of TPS micropulses of 1 s on the $AlCH_3$* surface at 175 °C with a delay time of 30 s. The TMA exposure of 2 s initiates the pulse sequence at $t = 0$. The first TPS exposure of 300 mTorr at $t = 32$ s displays the largest mass gain of all the TPS micropulses. The second TPS exposure at $t = 63$ s yields a smaller mass gain. The subsequent TPS

(30) Smith, D. L. *Thin-Film Deposition: Principles and Practice*: McGraw-Hill: New York,1995; Chapter 13.

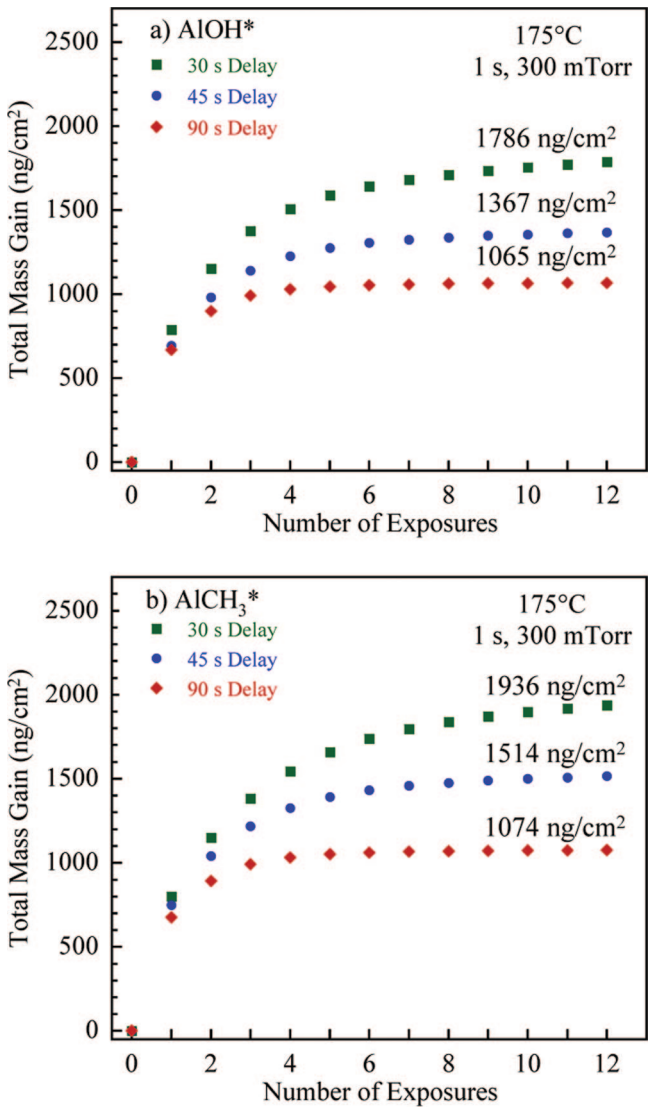

Figure 6. Total mass gain after a series of 1 s TPS micropulses at 175 °C with different delay times between the TPS micropulses using 300 mTorr TPS pressures on: (a) AlOH* terminated surface; (b) $AlCH_3$* terminated surface.

micropulses produce progressively smaller mass gains until the total mass gain asymptotically reaches a limit after 11−12 micropulses. The total mass gain resulting from all the TPS micropulses is 1936 ng/cm^2. Qualitatively similar results were observed earlier for undersaturating TBS micropulses at 250 °C.[19]

The effect of the various delay times between subsequent TPS exposures on AlOH* surfaces is displayed in Figure 6a. An overall mass gain of 1065 ng/cm^2 was observed for a 90 s delay time between the TPS micropulses. The mass gain reached completion by the fourth TPS micropulse. The total reaction time through the end of the fourth cycle was 364 s. When a 45 s delay time was used between the TPS micropulses, a larger total mass gain of 1367 ng/cm^2 was observed, and the mass gain was saturated by the seventh TPS micropulse after a total reaction time of 322 s. The 30 s delay time between TPS micropulses had an even larger overall mass gain of 1786 ng/cm^2. The growth did not saturate until the 15th micropulse with a total reaction time of 240 s.

Figure 6b shows the mass gains for the $AlCH_3$* starting surfaces. The 90 s delay time between TPS micropulses leads to a mass gain of 1074 ng/cm^2 that saturated by the fourth micropulse exposure. For the 45 s delay times, the mass gain saturates at 1514 ng/cm^2 after the seventh micropulse. This mass gain was noticeably higher by ∼150 ng/cm^2 than the mass gain observed on the AlOH* starting surface for similar micropulse exposure conditions. Lastly, the 30 s delay times between TPS micropulses saturated at 1936 ng/cm^2 after the 15th micropulse. This mass gain was also 150 ng/cm^2 higher than the mass gain observed on the surface with AlOH* species.

The similarity between the results in Figure 6a,b indicates that TPS can react with both AlOH* and $AlCH_3$* surface species. TPS can continue to insert into the Al catalytic center left from either the AlOH* or $AlCH_3$* surface species. The first 300 mTorr micropulse of TPS led to a mass gain of ∼700 ng/cm^2 as shown in Figure 6a,b. These results agree with the previous single exposure results shown in Figure 2. In addition, the mass gain was observed to decrease for each subsequent TPS micropulse on surfaces covered with either AlOH* and $AlCH_3$* initial species.

The decrease of the mass gain with each subsequent micropulse of TPS is expected because of the growing diffusion barrier for incoming TPS monomers. The barrier develops as the SiO_2 film grows and the siloxane chains cross-link by forming Si−O−Si linkages. Increasing the delay time between TPS micropulses revealed an additional decrease of the mass gain. This additional decrease is also attributed to a more effective diffusion barrier. In this case, the improved diffusion barrier resulted from more cross-linking reactions that form a denser SiO_2 film during the longer delay times and limit the amount of TPS monomers that reach the Al catalytic centers.

D. Continuous Exposure Experiments. The multiple exposure experiments with variable delay times indicated that the thickest SiO_2 films should be deposited using continuous exposures. The timing sequence for the continuous exposure experiments was 2−30−400−600. Much lower TPS pressures of 25 and 40 mTorr were investigated using the continuous exposure experiments. The TPS bubbler temperature for these experiments was maintained at 82 and 90 °C for TPS pressures of 25 and 40 mTorr, respectively. The TPS exposures of 400 s were sufficient for the SiO_2 film growth to reach saturation at all temperatures. The use of a purge of 600 s was predominately for the QCM experiments to avoid any SiO_2 chemical vapor deposition (CVD) following the 400 s TPS exposures. The same conditions were used for both the QCM and XRR investigations.

Figure 7 displays the mass gain during continuous exposures of 400 s at TPS pressures of 25 mTorr from 125−250 °C. The TPS exposures begin at $t = 0$ s. The temperature dependence observed in Figure 7 is very dramatic. These results agree well with the temperature dependence observed during the single exposure experiments in Figure 2. In addition, an expanded view of the initial stages of the mass gain from the start of the TPS exposure is shown in Figure 8. Large variations were observed for the initial

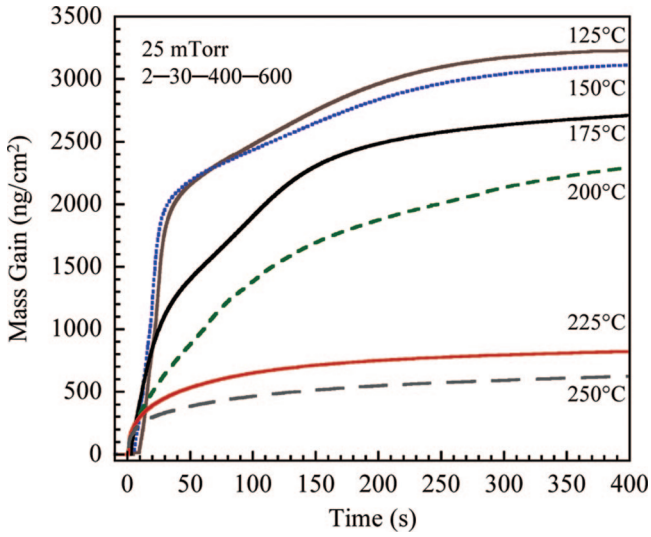

Figure 7. Mass gain versus time from the start of the TPS exposure during continuous TPS exposures at various substrate temperatures using a TPS pressure of 25 mTorr.

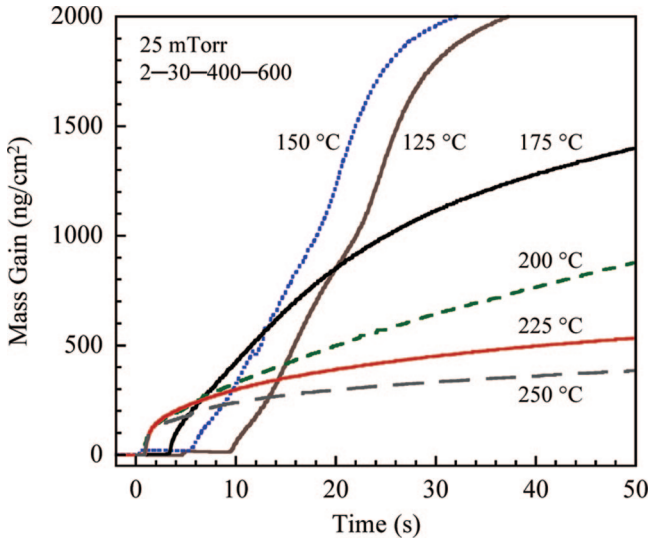

Figure 8. Expansion of the early time region of Figure 7 showing the mass gain versus time from the start of the TPS exposure during continuous TPS exposures at various substrate temperatures using a TPS pressure of 25 mTorr.

silanol reaction and silanol insertion. Figure 8 shows that delays of 3, 5, and 8 s were observed for 175, 150, and 125 °C, respectively. The delay can be attributed to a decrease in the kinetics of the insertion reaction. Alternatively, the delay could be caused by increased reactivity for the TPS and a majority of the TPS being consumed on the reactor walls before reaching the QCM.[31]

Figures 7 and 8 reveal three temperature regions. The low temperature region at ≤150 °C is characterized by a delayed nucleation for the silanol reaction, a rapid silanol insertion reaction, and a slow termination or cross-linking reaction. For the intermediate temperatures at 175−200 °C, the initial silanol reaction was faster than the initial silanol reaction observed at lower temperatures. However, following the initial silanol reaction, the silanol insertion rates were much

(31) Hausmann, D. M.; Kim, E.; Becker, J.; Gordon, R. G. *Chem. Mater.* **2002**, *14*, 4350.

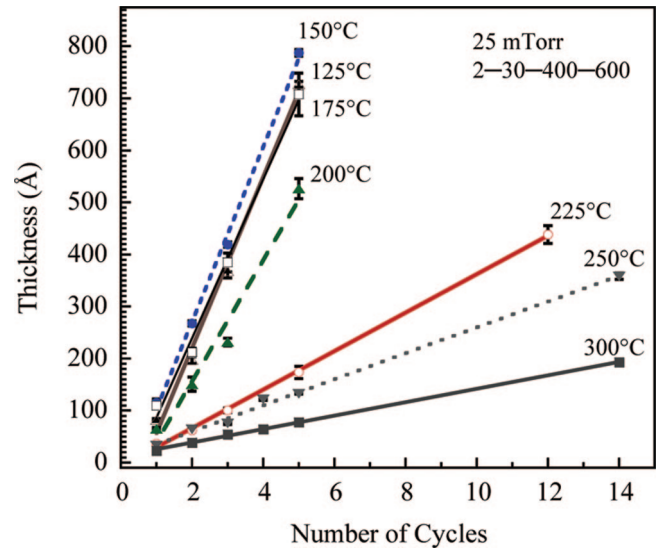

Figure 9. Film thickness versus number of cycles on Si(100) substrates at various substrate temperatures using continuous TPS exposures of 400 s and TPS pressures of 25 mTorr.

less than the silanol insertion rates observed in the low temperature region. This behavior is presumably caused by faster cross-linking reactions that limit the silanol insertion at intermediate temperatures. The high temperature region of ≥225 °C was characterized by a very rapid initial silanol reaction and also rapid silanol insertion and cross-linking reaction rates. A consequence of these faster reaction rates was much lower overall deposition resulting from the fast cross-linking that terminates the SiO_2 growth.

XRR investigations were also employed to characterize the results for the continuous TPS exposures. One, two, three, and five rapid SiO_2 ALD cycles were deposited at 125, 150, 175, and 200 °C using TPS pressures of 25 mTorr. Because of the lower deposition rates at higher temperatures, 12, 14, and 24 rapid SiO_2 ALD cycles were utilized at 225, 250, and 300 °C, respectively. The XRR results for film thickness versus number of rapid SiO_2 ALD cycles are shown in Figure 9. The thickness deposited per cycle decreases progressively with increasing temperature.

The error bars in Figure 9 result from the variation of the SiO_2 film thickness versus position in the reactor for three separate samples. At low temperatures of 125 and 150 °C, there was no dependence of film thickness on position. This observation argues that the delays in nucleation observed in Figure 8 result from a reduction in the silanol insertion kinetics instead of the consumption of the reactant prior to the QCM. Much larger variations in film thickness are observed at intermediate temperatures of 175, 200, and 250 °C. This variation could be caused by the upstream consumption of reactant that would lead to nonuniform reactant concentrations and variable film thicknesses. In the high temperature region at 250 and 300 °C, the position dependence of the film thickness was again negligible. Although the reaction rates are increased at higher temperatures, the consumption of the reactant is lower at higher temperatures because polymer cross-linking more readily produces self-limiting growth and thinner SiO_2 films. Lower reactant consumption at these higher temperatures yields a more

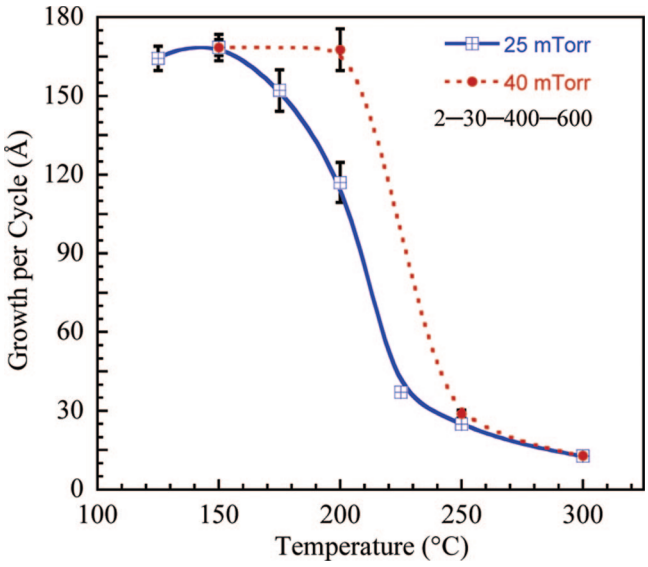

Figure 10. Growth per cycle at various substrate temperatures using 25 mTorr and 40 mTorr continuous TPS exposures of 400 s.

uniform reactant concentration throughout the reactor and negligible position dependence.

A summary of the rapid SiO_2 ALD growth per cycle versus temperature for the continuous TPS exposures at 25 mTorr from Figure 9 is displayed in Figure 10. A set of samples was also deposited at 150, 200, 250, and 300 °C using continuous TPS exposures at 40 mTorr. These experiments explored the dependence of the growth per cycle on TPS pressure. The growths per cycle for the continuous TPS exposures at 40 mTorr are also shown in Figure 10.

In the low temperature region at ≤150 °C, Figure 10 shows that the growth per cycle was between 165−170 Å using the 25 mTorr exposures. The increase of the TPS pressure to 40 mTorr had no effect on the SiO_2 growth rate at 150 °C. The lack of pressure dependence at 150 °C indicates that the rapid SiO_2 ALD is in a kinetic-limited regime. The catalytic Al centers are saturated with TPS monomers. Changes in the flux of incoming TPS monomers do not effect the deposition rate. The lack of pressure dependence may indicate the existence of a silanol multilayer at these low temperatures that acts as a reservoir for reactant molecules. In addition, no thickness gradient was observed with respect to position in the reactor at the low temperatures. These results confirm that the pressure was sufficient to maintain Al catalytic centers saturated with reactant throughout the reactor.

In the intermediate temperature region at 175 and 200 °C, Figure 10 shows that the growth per cycle using 25 mTorr TPS exposures decreased to 152 and 117 Å, respectively. In addition, a much larger gradient in film thicknesses was observed with the thickest samples being closest to the incoming silanol reactant flux. The gradient may be a consequence of the incoming reactant flux being consumed and results in lower downstream reactant fluxes. In support of this explanation, higher growth per cycle was observed at 40 mTorr. Figure 10 indicates that the growth per cycle at 200 °C and 40 mTorr rose to 167 Å. The higher growth per cycle at higher reactant pressures argues that the growth is flux-limited. In addition, slightly different thicknesses were also observed at different spatial positions with the thicker films observed closest to the incoming reactant flux. These results at 40 mTorr again support the explanation that the reactant flux is being depleted during its passage through the reactor.

Figure 10 also shows that the growth per cycle was much lower at high temperatures of 225, 250, and 300 °C. The growth per cycle dropped from 37 to 12 Å from 225 to 300 °C using 25 mTorr exposures. However, a gradient in film thicknesses with spatial position in the reactor was not observed at these high temperatures. On the basis of the QCM investigations, the propagation and cross-linking rates were much faster in the high temperature region and led to much lower overall mass gains. Less TPS reactant is consumed, and reactant depletion is not a problem. In this high temperature region, the initial incoming TPS flux has only a minimal effect on the growth per cycle. The increase in the reactant pressure from 25 to 40 mTorr at 250 °C only resulted in an increase in the growth per cycle from 25 to 29 Å.

The film roughness was also dependent on deposition temperature for the SiO_2 films grown using continuous exposure. At low growth temperatures ≤ 150 °C, the film roughnesses observed by XRR were much lower than the square root of the film thickness. For example, a 720 Å film deposited at 125 °C showed a roughness of 18 Å. A 785 Å film deposited at 150 °C showed a surface roughness of only 22 Å. In contrast, at higher temperatures ≥ 175 °C, the SiO_2 film roughnesses scaled with the square root of the film thickness as expected for a random deposition process.[30] This contrast in surface roughness versus temperature indicates that there are unique conditions at low temperatures that produce very smooth SiO_2 films. The extremely smooth SiO_2 films at low temperatures support the explanation that a reactant multilayer may be present at lower temperatures. The multilayer may eliminate the randomness of the deposition by maintaining a constant reservoir of silanol monomers on the surface.

The XRR investigations also yielded the density of the deposited SiO_2 films. These densities are displayed in Figure 11 together with the growth per cycle for the TPS exposures at 25 mTorr. The film density in the low temperature region at ≤150 °C was ∼2.02 g/cm^3. When the deposition temperature increased to 175 °C, the density increased to ∼2.1 g/cm^3. The density then increased further to ∼2.15 g/cm^3 at ≥200 °C. For comparison, the SiO_2 film density obtained from wet and dry thermal oxidation of silicon is 2.2 g/cm^3.[32] Figure 11 illustrates that the change observed in film density occurs in the intermediate temperature region. This increase in film density may be expected based on the increase in the cross-linking rate that yields denser SiO_2 films. Another consequence of the increased cross-linking rate and larger film density is the smaller growth per cycle observed at >150 °C.

FTIR spectroscopy was used to monitor the vibrational spectrum of SiO_2 ALD films grown on the surface of the ZrO_2 particles at 150 °C versus TPS exposure. Before the

(32) Petersen, K. E. *IEEE Trans. Electron Devices* **1978**, *35*, 1241.

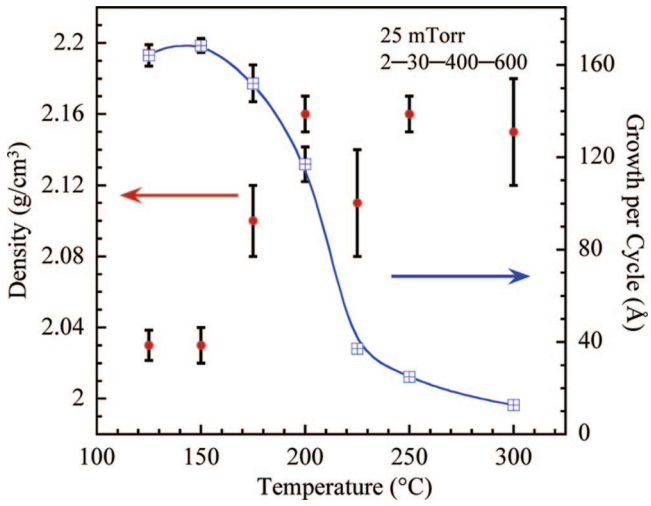

Figure 11. Density of SiO_2 films at various substrate temperatures using 25 mTorr continuous TPS exposures of 400 s. Density is compared with growth per cycle at various substrate temperatures using continuous 25 mTorr TPS exposures of 400 s.

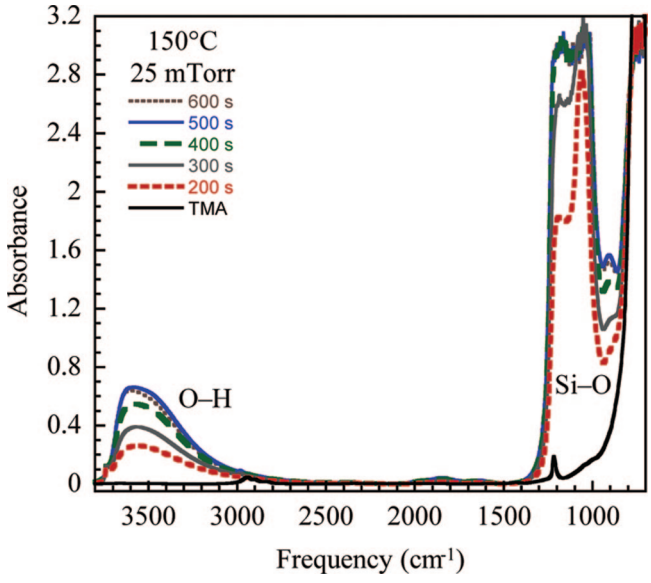

Figure 12. FTIR vibrational spectra after TMA exposure and after TPS exposures of 200, 300, 400, 500, and 600 s at TPS pressure of 25 mTorr at 150 °C.

TPS exposure, 10 cycles of Al_2O_3 ALD were performed using TMA and H_2O to yield a reproducible starting surface. The last TMA exposure left a surface covered with $AlCH_3$* species. Figure 12 shows the FTIR spectra during a TPS exposure of 25 mTorr. The results agree with the previous QCM experiments and show that TPS exposures at 25 mTorr for >400 s approach saturation. Slightly longer exposure times are needed to reach saturation because the ZrO_2 particles used to enhance the surface area have a lower gas conductance.

Figure 12 shows that the starting surface has CH_x features located at 2700−3000 cm^{-1} and 1215 cm^{-1} due to C−H stretching and deformation modes, respectively, of the $AlCH_3$* species from TMA exposures. Following the initial TPS exposures of 200 s, a dramatic increase in the absorbance of Si−O bulk vibrations was observed at 1100−1300 cm^{-1}. There is also an increase in the absorbance of O−H stretching vibrations at 3000−3700 cm^{-1}. In addition, a decrease in the absorbance of the C−H stretching vibrations is observed at 2700−3000 cm^{-1}. These results agree with the removal of $AlCH_3$* species and the growth of a SiO_2 film. The growth of absorbance of O−H stretching vibrations results from the incomplete removal of SiOH* species at low temperature. These hydroxyl groups left in the film lead to the lower film density at low temperatures.

Table 1. RBS and ERD (Hydrogen) Results for SiO_2 Films with a Thickness of ~400 Å Deposited at 125−300 °C Using TPS with ~0 ppm Impurity Level and a Timing Sequence of 2−30−400−600

	Si	O	C	H	Si:O
125 °C	0.30	0.61	<0.01	0.09	0.49
150 °C	0.32	0.64	<0.01	0.04	0.50
175 °C	0.31	0.62	<0.01	0.06	0.50
200 °C	0.32	0.64	0.01	0.03	0.50
225 °C	0.31	0.62	0.015	0.06	0.50
250 °C	0.28	0.62	0.02	0.09	0.45
300 °C	0.26	0.57	0.03	0.14	0.46

E. Composition of Rapid SiO_2 ALD Films. RBS and ERD were used to investigate the composition of rapid SiO_2 ALD films grown at 125−300 °C. For this analysis, three cycles of rapid SiO_2 were deposited at 125, 150, and 175 °C. For rapid SiO_2 ALD at 200, 225, 250, and 300 °C, the number of cycles was 5, 12, 14, and 24, respectively. The various cycle numbers at different temperatures were used to obtain film thicknesses of ~400 Å for more consistent RBS analysis. Table 1 gives the RBS results for films deposited at 125−300 °C. The uncertainty for the C atomic fraction was <0.01 because nuclear reaction analysis was used in combination with RBS to enhance the sensitivity. The uncertainty for the H atomic fraction based on the ERD analysis was also <0.01.

At all deposition temperatures below 225 °C, carbon was below the detection limit. These results are in agreement with the FTIR results that indicated a minimal amount of absorbance from C−H_x vibrational features after TPS exposures. The carbon levels increased slightly with deposition temperature at 225−300 °C. This increase is most likely caused by the decomposition of TPS. This decomposition is also confirmed by the increase in hydrogen observed at these higher temperatures. The hydrogen may result from the presence of CH_x decomposition species.

Si/O ratios of <0.50 were observed above 225 °C. This deviation from a Si/O ratio of 0.50 indicates the films are oxygen rich or silicon deficient and probably is related to the decomposition of TPS. The amount of hydrogen in the films was highest at 125 °C and 250−300 °C. The increase in hydrogen at lower temperatures is expected based on slow cross-linking reactions that lead to higher concentrations of hydroxyl species. These hydroxyl species are observed in the FTIR spectra in Figure 12. The higher hydroxyl coverages also correlate with the lower SiO_2 film densities observed in Figure 11.

The SiOH* species were stable in the SiO_2 films following rapid SiO_2 ALD at 150 °C. The time dependence of the FTIR spectra of SiO_2 films grown at 150 °C and then annealed at 200 °C is displayed in Figure 13. The hydroxyl coverage is slowly lost versus time as the SiOH* species recombine with each other to produce H_2O according to the reaction given

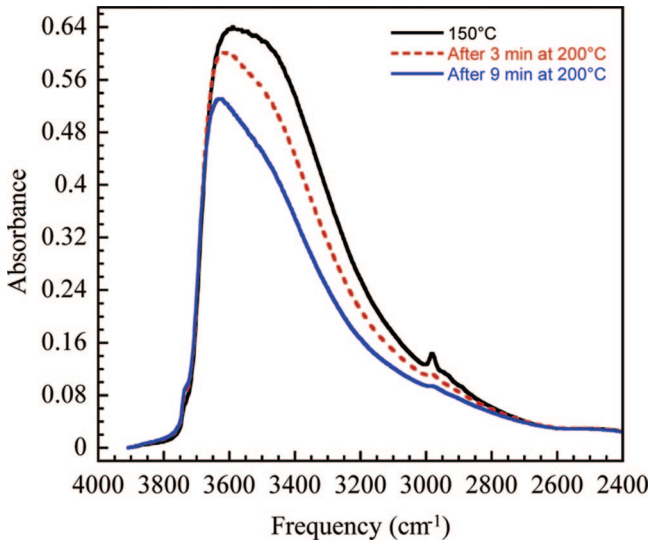

Figure 13. FTIR spectra in the O−H stretching vibration region for a SiO_2 film grown at 150 °C and then after annealing for 3 and 9 min at 200 °C.

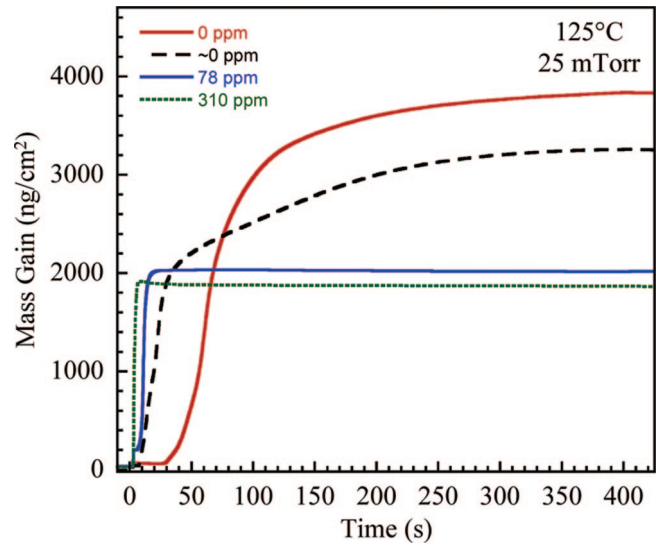

Figure 14. Mass gain versus time from the start of the TPS exposure during continuous TPS exposure at 125 °C using a TPS pressure of 25 mTorr. Results are shown for four different TPS samples with 0, ~0, 78, and 310 ppm of tris(*tert*-pentoxy)silylpyridine impurity.

by eq 5. This loss of hydroxyls at 200 °C through the cross-linking reaction is expected to lead to the larger film densities observed in Figure 11 at higher temperatures.

F. Effect of Tris(*tert*-pentoxy)silylpyridine) Impurity. During the course of these experiments, we learned from SAFC Hitech that TPS could contain pyridine derivatives such as tris(*tert*-pentoxy)silylpyridine in trace concentrations depending on the synthetic route used for TPS production. Tris(*tert*-pentoxy)silylpyridine was identified by gas chromatography−mass spectrometry (GC-MS) analysis. The GC-MS analysis did not provide information on the exact isomer. The pyridine derivatives were believed to influence the growth of the rapid SiO_2 ALD films.

Subsequent investigations revealed that pyridine and substituted pyridines alter the kinetics of rapid SiO_2 ALD film growth. The effect of pyridine and substituted pyridines was not unexpected because SiO_2 ALD can be influenced by Lewis base catalysts.[8−12] Previous work showed that SiO_2 ALD using $SiCl_4$ and H_2O requires temperatures of >325 °C and reactant exposures of $>1 \times 10^9$ L.[6] The required temperatures are reduced to around room temperature, and the necessary exposures are lowered to 10^4 L in the presence of a Lewis base in the form of NH_3 or pyridine.[8−12]

Experiments were conducted to determine the effect of pyridine on rapid SiO_2 ALD. In these experiments, rapid SiO_2 ALD was first monitored at 125 °C by QCM using continuous TPS exposures. After three cycles of rapid SiO_2 ALD, an exposure of pyridine was introduced following the TMA exposure. The pyridine exposure resulted in a pronounced reduction in the overall mass gain during the next TPS exposure. The mass gain following the pyridine exposure was around 30% of the mass gain in the absence of the pyridine exposure. This behavior suggests that the pyridine can modify the kinetics of the reactions given in eqs 1−5. Alternatively, the pyridine can bind to and modify the Al catalytic center.

Pyridine derivatives such as tris(*tert*-pentoxy)silylpyridine can also affect the growth and kinetics of rapid SiO_2 ALD using TPS. Various batches of TPS were obtained from SAFC Hitech that had 310 ppm, 78 ppm, and ~0 ppm of the tris(*tert*-pentoxy)silylpyridine in the TPS. These batches of TPS were prepared using the same synthetic strategy. In addition, another synthetic route that prevents the formation of tris(*tert*-pentoxy)silylpyridine yielded a batch of TPS that contained 0 ppm of tris(*tert*-pentoxy)silylpyridine.

Rapid SiO_2 ALD was then conducted using these four silanol samples at 125 °C using the continuous exposure experiments with a TPS pressure of 25 mTorr and the timing sequence of 2−30−400−600. These results are shown in Figure 14. The TPS exposures begin at time $t = 0$ s. In agreement with the preliminary results using pyridine, the total mass gain decreased with increasing impurity concentrations. However, Figure 14 also shows an increase in the nucleation of the rapid SiO_2 ALD at the higher impurity concentrations. The highest impurity level of 310 ppm nucleated the most rapidly at ~1 s after the initiation of the TPS exposure. The mass gain then terminated at a total mass gain of ~1900 ng/cm^2. The impurity concentration of 78 ppm showed the next fastest nucleation at ~3 s after the initiation of the TPS exposure. The main gain then leveled off at a total mass gain of ~2000 ng/cm^2.

The impurity concentration of ~0 ppm displayed the next fastest nucleation at ~8 s after the initiation of the TPS exposure. This TPS exposure then reached much higher total mass gains of ~3250 ng/cm^2 at TPS exposure times > 400 s. These results agree with the previous continuous exposure experiments in Figure 7. Finally, the impurity concentration of 0 ppm that was synthesized by a second route that prevents the formation of tris(*tert*-pentoxy)silylpyridine showed the longest nucleation time of ~28 s after the initiation of the TPS exposure. However, the total mass gain observed from the TPS with 0 ppm of impurity then reached the highest total mass gain of ~3800 ng/cm^2 at TPS exposures > 400 s.

The SiO_2 thicknesses deposited using the TPS batches with various levels of impurity were examined using XRR after various numbers of rapid SiO_2 ALD cycles at 125 °C for TPS pressures of 25 mTorr. The SiO_2 film thicknesses versus

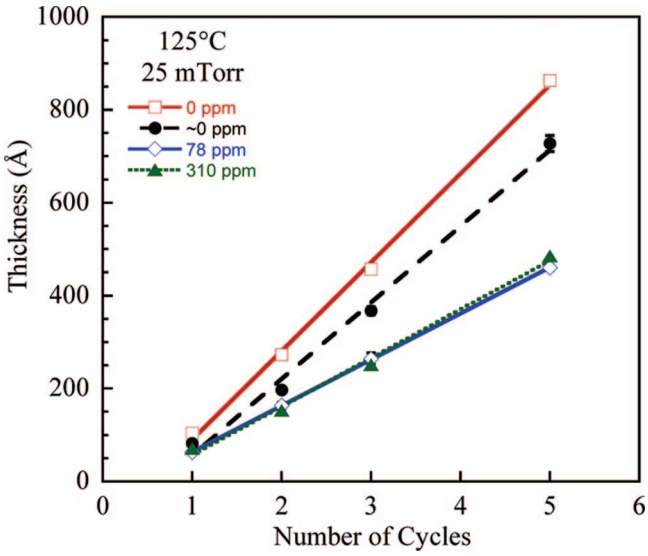

Figure 15. Film thickness versus number of cycles on Si(100) substrates at 125 °C using continuous TPS exposures of 400 s and TPS pressures of 25 mTorr. Results are shown for four different TPS samples with 0, ~0, 78, and 310 ppm of tris(*tert*-pentoxy)silylpyridine impurity.

the number of cycles are shown in Figure 15. These XRR results agree with the QCM results in Figure 14. The TPS with impurity levels of 310 and 78 ppm show a SiO_2 growth per cycle of ~100 Å based on a linear fit to the XRR data. The TPS with an impurity concentration of ~0 ppm yielded a SiO_2 growth per cycle of 165 Å. The TPS with an impurity level of 0 ppm displayed the largest SiO_2 growth per cycle of 191 Å.

The effect of pyridine derivatives on the growth of the rapid SiO_2 ALD films is believed to be caused by the catalytic effect of the Lewis base on both the silanol reaction that initiates the rapid SiO_2 ALD and the cross-linking reaction that limits the rapid SiO_2 ALD. The Lewis base impurities could facilitate the silanol reaction by hydrogen bonding with the hydroxyl group on TPS and making the oxygen a stronger nucleophile to attack the $AlCH_3$* surface species or insert at the Al catalytic center as given by the reactions in eqs 2 and 3.[11,12] Likewise, the Lewis base impurities could facilitate the cross-linking reaction by hydrogen-bonding with the hydroxyl group on SiOH* and making the oxygen a stronger nucleophile to promote the dehydration reaction in reaction given by eq 5.[11,12]

SiO_2 films grown at 150 °C using the TPS batch with the highest impurity concentration of 310 ppm were investigated by FTIR spectroscopy. The FTIR spectra were almost identical for SiO_2 films grown using the TPS with either ~0 ppm or 310 ppm of impurity. The FTIR spectra did reach completion more rapidly for the SiO_2 films grown using TPS with the highest impurity concentration of 310 ppm. The more rapid completion of the rapid SiO_2 ALD growth with the higher level of impurity is in agreement with the QCM results in Figure 14. The TPS with 310 ppm of impurity did yield a slightly larger amount of C−H vibrational features in the SiO_2 film. However, no vibrational features were attributed to the tris(*tert*-pentoxy)silylpyridine impurity. Pyridine was dosed onto the surface following these experiments to identify vibrational modes consistent with pyridine.

Table 2. RBS and ERD (Hydrogen) Results for SiO_2 Films with a Thickness of ~400 Å Deposited at 125 °C Using TPS with 0 ppm, ~0 ppm, and 310 ppm Impurity Levels and a Timing Sequence of 2−30−400−600

	Si	O	C	H	Si:O
0 ppm	0.29	0.59	<0.01	0.12	0.49
~0 ppm	0.30	0.61	<0.01	0.09	0.49
310 ppm	0.29	0.63	<0.01	0.08	0.46

To investigate the effect of the impurity on SiO_2 film composition, RBS was used to investigate rapid SiO_2 ALD films grown at 125 °C using TPS with impurity levels of 310 ppm and ~0 ppm obtained from the same synthetic procedure and TPS with an impurity level of 0 ppm. To obtain approximately the same film thicknesses, the rapid SiO_2 ALD films grown using TPS with impurity concentrations of ~0 ppm and 0 ppm were deposited using three cycles. The rapid SiO_2 ALD films grown using TPS with impurity concentrations of 310 ppm were deposited using five cycles. The results of the RBS analysis are shown in Table 2. The uncertainties for the C and H atomic fractions were again <0.01.

The carbon concentrations were below the RBS detection limit in all of the samples. These results indicate that the small C−H vibrational features in the FTIR spectra must be minimal for the SiO_2 films grown using the TPS with 310 ppm of impurity. The RBS results also indicate that the amount of hydrogen is nearly identical for the SiO_2 films grown using TPS with ~0 ppm and 310 ppm of impurity. On the other hand, TPS with 0 ppm of impurity had a slightly higher amount of hydrogen. The only other difference observed in the RBS results is the slightly low Si/O ratio for the SiO_2 films grown using TPS with 310 ppm of impurity.

G. Position of the Al Catalyst. SIMS was also used to investigate the position of the Al catalyst following the rapid SiO_2 ALD at 125 °C. The SiO_2 films were grown using five rapid SiO_2 ALD cycles. The Al signal versus sputter time during depth-profiling of a SiO_2 film grown using TPS with 310 ppm of impurity is shown in Figure 16a. The Al signal versus sputter time in a SiO_2 film grown using TPS with ~0 ppm of impurity is shown in Figure 16b. Both parts a and b of Figure 16 show distinct oscillations of the Al signal versus sputter time that illustrate that the Al catalyst does not disperse itself uniformly in the SiO_2 film. Both parts of Figure 16 display five peaks corresponding to the five layers of the Al catalyst.

The five peaks in Figures 16a,b are approximately evenly spaced versus sputter time. The SiO_2 film in Figure 16b shows a greater separation of the peaks versus sputter time because larger SiO_2 film thicknesses are deposited using TPS with ~0 ppm of impurity compared with 310 ppm of impurity. The SiO_2 growths per cycle using TPS with ~0 ppm and 310 ppm of impurity were 104 and 165 Å/cycle, respectively. The Al catalyst is believed to remain localized at the interface during the deposition of each SiO_2 film during the five rapid SiO_2 ALD cycles. The width of the Al peaks versus sputter time is attributed to the finite resolution of SIMS analysis.

SIMS was also used to probe for nitrogen from the silanol impurity using SiN at mass 42. SIMS results from a rapid

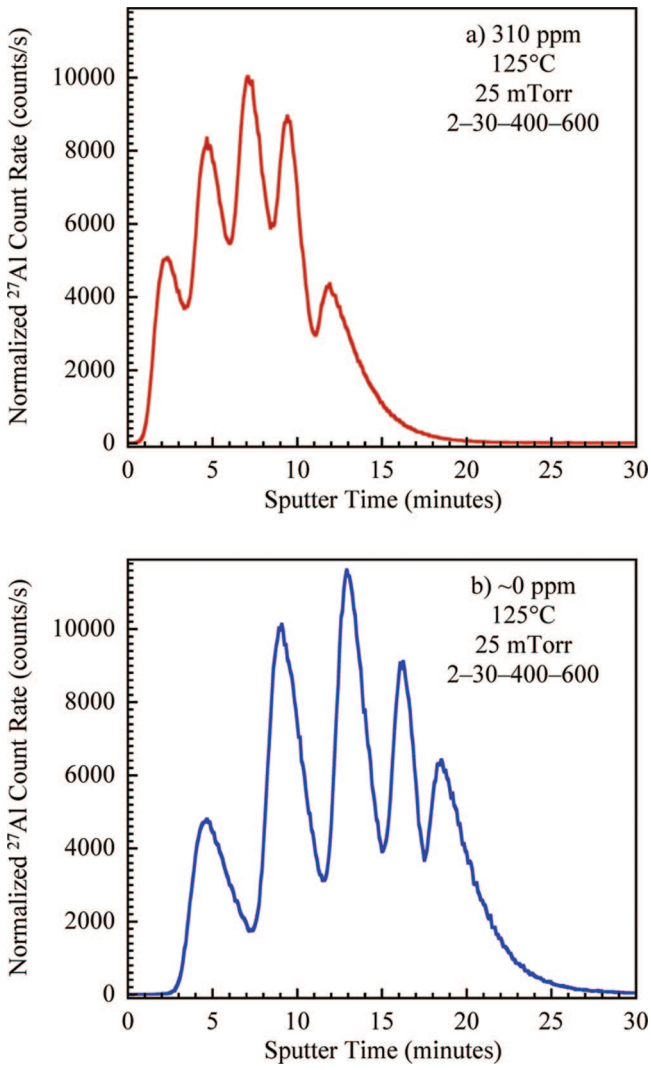

Figure 16. SIMS count rate for ^{27}Al during sputter depth profiling of SiO_2 films grown using five cycles with continuous TPS exposures of 400 s and TPS pressures of 25 mTorr at 125 °C. (a) TPS with ~0 ppm of tris(*tert*-pentoxy)silylpyridine impurity and (b) TPS with 310 ppm of tris(*tert*-pentoxy)silylpyridine impurity.

SiO_2 film deposited at 125 °C using TPS with 310 ppm of impurity showed a uniform distribution of nitrogen in the film. The analysis of a SiO_2 film deposited with ~0 ppm and 0 ppm of impurity also displayed signals at mass 42 that were much lower than the signal intensities observed using TPS with 310 ppm of impurity. These results suggest that remnants of the nitrogen-containing silanol impurity remain in the SiO_2 film at a uniform concentration.

H. Comparison between TBS and TPS for Rapid SiO_2 ALD and Catalytic Polymerization. The original report of rapid SiO_2 ALD summarized the proposed mechanism for rapid SiO_2 ALD using TBS in its Scheme 1.[19] This study of rapid SiO_2 ALD using TPS is in very close agreement with the general reaction mechanism in the original report. However, this study on TPS and the previous report on TBS differ in terms of the growth kinetics observed for TBS and TPS. Both investigations monitored self-limiting growth versus the silanol exposure. Substantial differences were observed for the reaction conditions that produced the optimum growth per cycle. The previous report observed a maximum in the TBS growth per cycle around 225−250 °C under their exposure conditions.[19] In contrast, this study measured the highest growth per cycle at the lowest temperatures of 125−150 °C.

The decrease in the growth per cycle at temperatures > 250 °C in the previous report using TBS was attributed to the higher cross-linking rates that limit the diffusion of silanol reactants through the growing film to the Al catalytic centers.[19] The results from this study using TPS are in agreement with this explanation. The decrease in the growth per cycle at temperatures < 225 °C for rapid SiO_2 using TBS was explained earlier in terms of the temperature dependence of the insertion/propagation reaction.[19] This study using TPS monitored a temperature dependence for the insertion/propagation reaction. However, the temperature dependence was observed for the nucleation time for SiO_2 growth after initiating the silanol exposure as shown in Figure 8.

Because the results in the previous report were conducted using finite TBS exposures, the possibility exists that the decrease in the growth per cycle at temperatures < 225 °C was observed because of the longer nucleation times required for growth at lower temperatures. Perhaps the growth per cycle using TBS would have been larger at lower temperatures if the TBS exposures had been longer than the reported 15 s exposures. The previous exposures were performed by allowing a 35 mL volume of TBS to expand into the deposition chamber.[19] The TBS pressure could have been continuously declining during the 15 s exposure. These decreasing TBS pressures may have affected the measured growth per cycle. The actual TBS pressures in the deposition reactor were not measured in the earlier studies.[19]

There are similarities between the growth of rapid SiO_2 ALD films and the growth of polymer films on supported metallocene catalysts.[33−35] During heterogeneous catalytic polymerization, polymers such as polypropylene are observed to grow on particles covered with metallocene catalysts. As the polymer layer grows in the induction period, the polymerization rate is observed to decrease progressively with time.[34] This decrease occurs because the polymer layer is a diffusion barrier to the incoming monomers that are attempting to reach the catalyst at the particle surface.[35] Prior to fragmentation that releases new active catalytic sites, the polymerization rate can decrease to nearly zero in similarity with the self-limiting rapid SiO_2 ALD growth.

Model studies of olefins on Ziegler−Natta catalysts have also displayed many of the same features as rapid SiO_2 ALD.[36−38] Because the $TiCl_x/MgCl_2$ and $TiCl_y$/Au catalysts remain at the substrate, the growing polypropylene and polyethylene polymer films form a diffusion barrier for the incoming monomers. The polymerization rates are observed to decrease resulting from monomer transport restrictions

(33) Alexiadis, A.; Andes, C.; Ferrari, D.; Korber, F.; Hauschild, K.; Bochmann, M.; Fink, G. *Macromol. Mater. Eng.* **2004**, *289*, 457.
(34) Knoke, S.; Korber, F.; Fink, G.; Tesche, B. *Macromol. Chem. Phys.* **2003**, *204*, 607.
(35) Zechlin, J.; Steinmetz, B.; Tesche, B.; Fink, G. H. *Macromol. Chem. Phys.* **2000**, *201*, 515.
(36) Kim, S. H.; Vurens, G.; Somorjai, G. A. *J. Catal.* **2000**, *193*, 171.
(37) Kim, S. H.; Tewell, C. R.; Somorjai, G. A. *Korean J. Chem. Eng.* **2002**, *19*, 1.
(38) Kim, S. H.; Somorjai, G. A. *Catal. Lett.* **2000**, *68*, 7.

through the polymer films.[36−38] By alternating the flux of propylene and ethylene monomers, these investigations have also confirmed that the active catalytic sites are localized at the substrate.[38]

IV. Conclusions

SiO_2 films have been grown using liquid tris(*tert*-pentoxy)silanol (TPS) to determine the growth kinetics and mechanism of rapid SiO_2 ALD. The SiO_2 film thicknesses were determined using quartz crystal microbalance and X-ray reflectivity measurements. The SiO_2 film thicknesses deposited during one silanol exposure were found to be dependent on the temperature, silanol pressure, and silanol exposure time. The SiO_2 ALD growth rate was larger at the lower temperatures and larger TPS pressures for TPS exposures of 1 s. SiO_2 ALD thicknesses of 125−140 Å were observed at the highest TPS pressures of ∼1 Torr at the lower temperatures of 150 and 175 °C.

The rapid SiO_2 ALD growth is thought to result from the growth of siloxane polymer chains at the Al-catalytic sites. The cross-linking of these polymer chains then forms a dense SiO_2 film. The results versus pressure indicated that higher TPS fluxes increase the siloxane polymerization rates. Likewise, the lower temperatures reduce the cross-linking rates between the siloxane polymers that self-limit the SiO_2 deposition. Experiments were conducted where small TPS micropulses were employed with different delay times between the micropulses to explore the rate of cross-linking between the siloxane polymers. The SiO_2 ALD thicknesses decreased with increasing delay times. This behavior suggested that the longer delay times produced more cross-linking that self-limits the SiO_2 deposition.

Experiments using continuous TPS exposures showed that higher temperatures produced faster nucleation of the rapid SiO_2 ALD. The nucleation was nearly immediate at the higher temperatures. In contrast, the nucleation could be as long as 10 s at the lower temperatures. The growth kinetics of rapid SiO_2 ALD could be understood in terms of the temperature dependence of nucleation and cross-linking and the pressure dependence of the siloxane polymerization rate. Additional investigations revealed that the rapid SiO_2 ALD was also dependent on the presence of pyridine derivatives in the TPS. These Lewis base impurities were found to catalyze both the initial nucleation and the cross-linking reaction during rapid SiO_2 ALD.

Acknowledgment. This work was supported by ASM, Inc., and ALD NanoSolutions. Some of the equipment employed in this work was provided by the National Science Foundation and the Air Force Office of Scientific Research. The authors are grateful to SAFC Hitech for providing the silanols. The RBS and ERD analysis was performed Ion Beam Analysis of Materials (IBeAM) in the LeRoy Eyring Center for Solid State Science at Arizona State University. The SIMS analysis was performed by Changwu Hu and Sanjay Patel at Evans Analytical Group.

CM801738Z